

Redox and complexation chemistry of the Cr^{VI}/Cr^V-D-galacturonic acid system

Juan C. González,^a Verónica Daier,^a Silvia García,^a Bernard A. Goodman,^b Ana M. Atria,^c Luis F. Sala^{*a} and Sandra Signorella^{*a}

^a Departamento de Química, Facultad de Ciencias Bioquímicas y Farmacéuticas, UNR, Suipacha 531, 2000, Rosario, Argentina. E-mail: inquirir@satlink.com; signorel@infovia.com.ar

^b Scottish Crop Research Institute, Invergowrie, Dundee, Scotland, UK DD2 5DA

^c Facultad de Ciencias Químicas y Farmacéuticas and CIMAT, Universidad de Chile, Casilla 233, Santiago, Chile

The oxidation of D-galacturonic acid by Cr^{VI} yields the aldaric acid and Cr^{III} as final products when a 30-times or higher excess of the uronic acid over Cr^{VI} is used. The redox reaction involves the formation of intermediate Cr^{IV} and Cr^V species, with Cr^{VI} and the two intermediate species reacting with galacturonic acid at comparable rates. The rate of disappearance of Cr^{VI}, Cr^{IV} and Cr^V depends on pH and [substrate], and the slow reaction step of the Cr^{VI} to Cr^{III} conversion depends on the reaction conditions. The EPR spectra show that five-coordinate oxo-Cr^V bischelates are formed at pH ≤ 5 with the uronic acid bound to Cr^V through the carboxylate and the α-OH group of the furanose form or the ring oxygen of the pyranose form. Six-coordinated oxo-Cr^V monochelates are observed as minor species in addition to the major five-coordinated oxo-Cr^V bischelates only for galacturonic acid : Cr^{VI} ratio ≤ 10 : 1, in 0.25–0.50 M HClO₄. At pH 7.5 the EPR spectra show the formation of a Cr^V complex where the *vic*-diol groups of Galur participate in the bonding to Cr^V. At pH 3–5 the Galur-Cr^V species grow and decay over short periods in a similar way to that observed for [Cr(O)(α-hydroxy acid)₂]⁻. The lack of chelation at any *vic*-diolate group of Galur when pH ≤ 5 differentiates its ability to stabilise Cr^V from that of neutral saccharides that form very stable oxo-Cr^V(diolato)₂ species at pH > 1.

Introduction

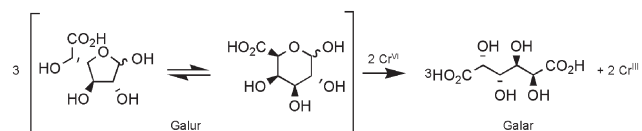
Compounds of Cr^{VI} represent a potential environmental hazard because of their mammalian toxicity and carcinogenicity.^{1–4} The observation of Cr^V and Cr^{IV} intermediates in the selective oxidation of organic substrates by Cr^{VI} and their implication in the mechanism of Cr-induced cancers^{1,5–7} has generated a considerable amount of interest in the chemistry and biochemistry of this element.^{8–13}

We are investigating the possible fate of Cr^{VI} and Cr^V in biological systems by examining reactions of Cr^{VI} with low-molecular-weight neutral^{14–26} and acid^{27–29} saccharides. Naturally occurring acid saccharides are suitable ligands for stabilization of Cr^V, since they possess the 2-hydroxycarboxylate and *vic*-diolate sites for potential chelation of Cr^V. Polygalacturonic acid is abundant in the primary cell walls of plants,³⁰ and galacturonic acid (Galur) is the major low-molecular-weight metabolite of pectic substances. The determination of the ability of Galur to reduce or stabilise high oxidation states of Cr, will contribute to unravel its potential role in the biochemistry of this metal. The reaction of Cr^{VI} with 1.5 equivalents of Galur has been studied previously by Branca and Micera.³¹ However, we have found that when the Galur to Cr^{VI} ratio is lower than 30, the oxidation product competes with Galur for Cr^{VI} so that degradation to the lower homologues occurs. Thus, several competitive reactions contribute to the kinetics and spectroscopic data obtained when Galur/Cr^{VI} ratios lower than 30 are used. It is then necessary to determine the ability of Galur to bind and reduce Cr^{VI} and Cr^V under conditions where interference from other reaction products is negligible as well as to assign the coordination modes of Galur in the Cr^V species formed in solution. In this work, we report the study of the redox reaction of Cr^{VI} with an excess of Galur (Scheme 1) in acidic medium and the ability of Galur to coordinate Cr^V generated in this reaction.

Results

Detection of Cr^V by EPR spectroscopy

The presence of Cr^V-Galur species can be identified with great sensitivity by EPR spectroscopy, where narrow isotropic signals are observed in spectra at room temperature. With a modulation ampli-



Scheme 1 Redox reaction of Cr^{VI} with excess of Galur.

tude of 4 G, the EPR spectra of solutions from the reaction between Cr^{VI} and Galur, consist of a major signal (from ⁵²Cr and other Cr isotopes with zero spin) centred at $g_{\text{iso}} = 1.9785$ (Fig. 1(a)), flanked by a weak quartet from the ⁵³Cr isotope ($I = 3/2$, natural abundance 9.5%). With lower modulation amplitude, there is clear resolution of the central peak into more than one component, as illustrated in Fig. 1(b) for a modulation amplitude of 0.29 G and $[\text{Cr}^{\text{VI}}]_0 = 2\text{--}3 \times 10^{-4}$ M. Changing $[\text{Galur}]$ did not affect the spectral resolution. The intensity of the EPR signal and the period over which Cr^V species could be observed was dependent on the $[\text{H}^+]$. When a large excess of Galur over Cr^{VI} was used ($\geq 30 : 1$), either in strongly acidic conditions (0.2–1.0 M HClO₄) or in the 1–5 pH range, the EPR spectra were composed of two triplets at $g_{\text{iso}1} = 1.9786$ ($a_{\text{H}} = 0.58(3) \times 10^{-4}$ cm⁻¹) and $g_{\text{iso}2} = 1.9784$ ($a_{\text{H}} = 0.98(3) \times 10^{-4}$ cm⁻¹), and one doublet at $g_{\text{iso}3} = 1.9785$ ($a_{\text{H}} = 0.79(3) \times 10^{-4}$ cm⁻¹). The presence of the weak ⁵³Cr hyperfine peaks with $A_{\text{iso}} = 17.2(1) \times 10^{-4}$ cm⁻¹ demonstrated that each of these components originated from Cr. These conclusions were also confirmed by performing additional EPR measurements on solutions from the reaction of Na₂⁵³CrO₄ with excess of Galur at several pH values.

In addition to the main signal centred at $g_{\text{iso}} = 1.9785$, the EPR spectra of the reaction of 2.0×10^{-3} M Cr^{VI} with a 10-times molar excess of Galur, in 0.50 or 0.75 M HClO₄, showed an additional weak signal at $g_{\text{iso}} = 1.972$ (Fig. 1(c)), whose relative intensity was ≤10% of the main signal. The signal at $g_{\text{iso}} = 1.972$ was not observed when the $[\text{Galur}] : [\text{Cr}^{\text{VI}}]$ ratio was increased to 20 : 1 or when the concentration of both Galur and Cr^{VI} were increased.

The EPR spectra of the reaction of 3.2×10^{-3} M Cr^{VI} with 0.24 M Galur in HEPES buffer (pH 7.5), with a modulation amplitude of 1.0 G, were dominated by a signal at $g_{\text{iso}} = 1.9793$.

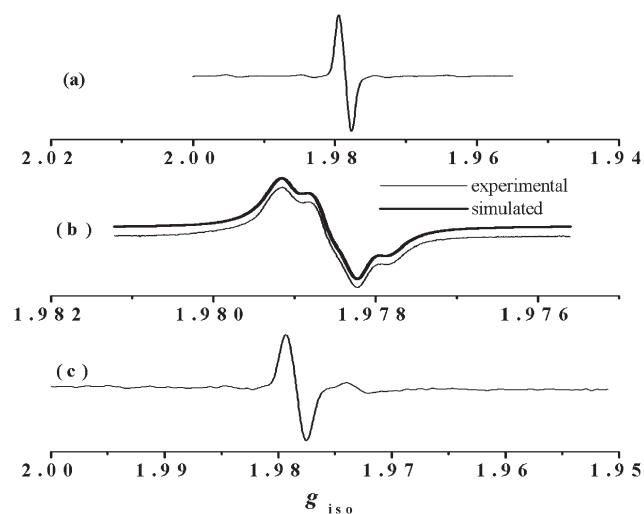


Fig. 1 X-Band EPR spectra from Cr^{VI} + Galur reaction mixtures. (a) $\text{Cr}^{\text{VI}}:\text{Galur} = 1:30$, $[\text{H}^+] = 0.20 \text{ M}$, mod. ampl. = 4.0 G; (b) $\text{Cr}^{\text{VI}}:\text{Galur} = 1:1900$, pH 3.0, mod. ampl. = 0.29 G; (c) $\text{Cr}^{\text{VI}}:\text{Galur} = 1:10$, $[\text{H}^+] = 0.75 \text{ M}$, mod. ampl. = 4.0 G; $T = 25 \text{ }^\circ\text{C}$, $I = 1.0 \text{ M}$, frequency $\approx 9.78 \text{ GHz}$.

At room temperature and pH 4–5, the reaction of Cr^{VI} with glutathione (1 : 1 ratio) in the presence of 400- to 1000-times molar excess of Galur produced Cr^{V} EPR spectra identical to those obtained by direct reaction of Cr^{VI} with Galur.

Until now, only Cr^{V} species formed with tertiary 2-hydroxy acids, such as $\text{Cr}^{\text{V}}(\text{ehba})_2$, $\text{Cr}^{\text{V}}(\text{hmba})_2$ (ehba = 2-ethyl-2-hydroxybutanoato(2-); hmba = 2-hydroxy-2-methylbutanoato(2-)), without carbinolic protons coupled to the Cr^{V} electron spin, have been fully characterised by EPR spectroscopy.³² In order to have a reference pattern for the superhyperfine structure (shfs) of the EPR signal of Cr^{V} species formed with secondary 2-hydroxy acid, we investigated the ligand shfs in EPR spectra of Cr^{V} -lactic acid and Cr^{V} -tartaric acid chelates. The EPR spectrum from a mixture of Cr^{VI} , glutathione and lactic acid (1 : 1 : 1700 ratio) at pH 4.5 is shown in Fig. 2(a). This could be fitted with two triplets at $g_{\text{iso}} = 1.9788$ ($a_{\text{H}} = 0.53(1) \times 10^{-4} \text{ cm}^{-1}$) and 1.9784 ($a_{\text{H}} = 0.59(1) \times 10^{-4} \text{ cm}^{-1}$), with $^{53}\text{Cr } A_{\text{iso}} = 17.3(1) \times 10^{-4} \text{ cm}^{-1}$. Tartaric acid behaved in a similar way, producing a spectrum composed of two triplets at $g_{\text{iso}} = 1.9784$ ($a_{\text{H}} = 0.49(2) \times 10^{-4} \text{ cm}^{-1}$) and 1.9782 ($a_{\text{H}} = 0.79(4) \times 10^{-4} \text{ cm}^{-1}$), with $^{53}\text{Cr } A_{\text{iso}} = 17.2(1) \times 10^{-4} \text{ cm}^{-1}$ (Fig. 2(b)), at pH 4.5 and 1 : 1 : 730 glutathione : Cr^{VI} : tartaric acid ratio. The same EPR spectrum was obtained by direct reaction of Cr^{VI} with tartaric acid at this pH. In HEPES buffer (pH 7.5) the reaction of glutathione and Cr^{VI} in the presence of lactic acid, did not produce any Cr^{V} -lactic acid species that could be detected by EPR.

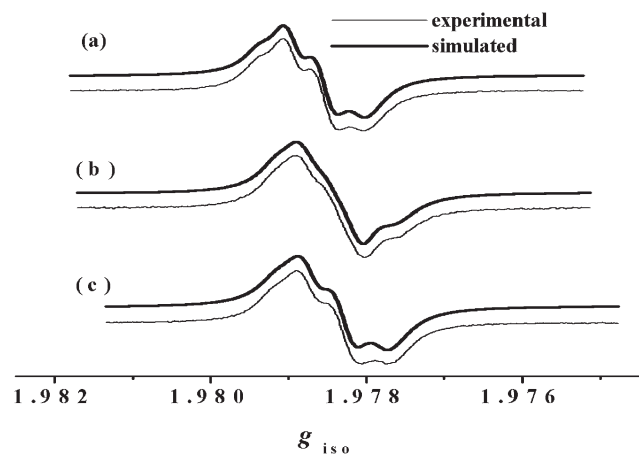


Fig. 2 Experimental and simulated X-band EPR spectra from mixtures of (a) glutathione : Cr^{VI} : lactic acid = 1 : 1 : 1700; (b) glutathione : Cr^{VI} : tartaric acid = 1 : 1 : 700; (c) glutathione : Cr^{VI} : Galur = 1 : 1 : 160; $T = 20 \text{ }^\circ\text{C}$, pH 4.5, mod. ampl. = 0.4 G, frequency $\approx 9.38 \text{ GHz}$.

The EPR spectral parameters of Cr^{V} -Galur species were also determined, because Galur formed in the oxidation of Galur by Cr^{VI} could in principle contribute to the EPR signal observed in the reaction mixtures. The EPR spectrum (Fig. 2(c)) of the reaction of glutathione with Cr^{VI} in the presence of Galur (1 : 1 : 158), at pH 4–5, contained two triplets at $g_{\text{iso}} = 1.9780$ ($a_{\text{H}} = 0.67 \times 10^{-4} \text{ cm}^{-1}$) and 1.9785 ($a_{\text{H}} = 0.53 \times 10^{-4} \text{ cm}^{-1}$).

In all of these reactions, the ultimate fate of the chromium was a Cr^{III} species and a typical broad Cr^{III} EPR signal centred at $g \sim 1.98$ was always observed during the later stages of the measurements.

Detection of Cr^{VI} esters

Differential UV/vis spectra of mixtures of Cr^{VI} and Galur exhibited two absorption bands with $\lambda_{\text{max}} = 360$ and 387 nm (Fig. 3), consistent with those ascribed to Cr^{VI} oxy esters.^{33,34} At pH 6.5, the redox reaction proceeded slowly with only a small reduction of $[\text{Cr}^{\text{VI}}]$ being observed during the first minutes. Thus, at this pH the ester formation step can be distinguished clearly from the electron transfer reaction at short reaction times. The intensities of these bands decreased over 15 min but the spectral pattern was retained. The absorbance of these two bands increased with increasing concentration of Galur when the $[\text{Galur}]$ was varied at pH = 6.5, probably as a result of a shift toward the ester in the esterification equilibrium. Furthermore, the relative intensities of the two bands ($\lambda_{360}/\lambda_{387}$) varied from 0.5 to 0.8 with increasing $[\text{Galur}]$, indicating that they correspond to two different Cr^{VI} -Galur species.

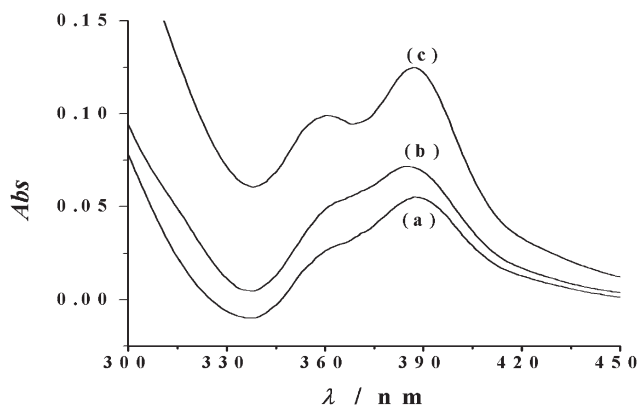


Fig. 3 UV/vis difference spectra of Cr^{VI} + Galur solutions at pH 6.5, showing the increasing bands at 360 and 387 nm with increasing $[\text{Galur}]$: (a) 0.032, (b) 0.047 and (c) 0.60 M; $[\text{Cr}^{\text{VI}}] = 6.1 \times 10^{-4} \text{ M}$, $T = 27 \text{ }^\circ\text{C}$, $I = 2.0 \text{ M}$. Spectra taken 2 min after preparation of solutions.

Intermediacy of Cr^{II}

It is known that Cr^{IV} oxidises alcohols as a two-electron oxidant to yield Cr^{II} and the oxidised organic product.^{35–39} The participation of Cr^{II} in the mechanism of the oxidation of several alcohols by Cr^{IV} and Cr^{VI} in HClO_4 has been demonstrated by conversion to CrO_2^{2+} upon reaction with molecular oxygen.^{35–39} At high $[\text{O}_2]$ and low $[\text{Cr}^{\text{VI}}]$ the reaction of Cr^{II} with O_2 can compete successfully with the reaction of Cr^{II} with Cr^{VI} and the autocatalytic consumption of CrO_2^{2+} by Cr^{II} , and if formed, Cr^{II} should yield the CrO_2^{2+} product.^{35,36,40} We examined the presence of intermediate Cr^{II} in the reaction of Galur with Cr^{VI} , by monitoring the formation of CrO_2^{2+} , using a $[\text{Cr}^{\text{VI}}]_0$ lower than employed in the kinetic studies. A periodic scanning of the O_2 -saturated solution (1.26 mM O_2) of a Cr^{VI} + Galur reaction mixture in 2.0 M HClO_4 showed two absorption bands at 290 and 247 nm characteristic of CrO_2^{2+} (Fig. 4). These spectroscopic results reveal that Cr^{II} forms in the redox reaction, and can be taken as evidence that Cr^{IV} is implied in the redox mechanism of the reaction between Cr^{VI} and Galur.

Rate studies

The reaction of Galur with Cr^{VI} in the 1.0–0.2 M HClO_4 used in kinetic measurements, produced an absorbance band at 350 nm and a shoulder at 420–500 nm, characteristic of Cr^{VI} in acidic medium, in the time-dependent UV/vis spectra. Rate constants were calculated

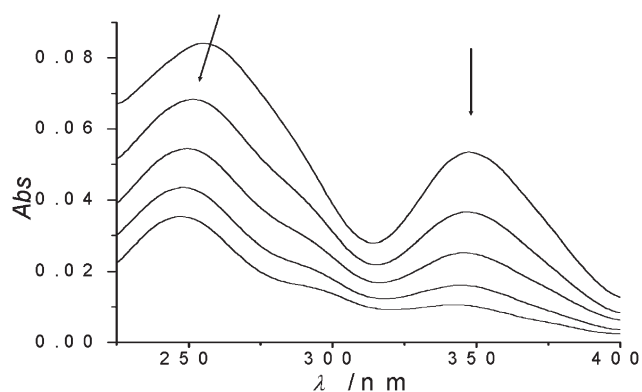


Fig. 4 Formation of CrO_2^{2+} (λ_{max} 290, 249) from the reaction between 42 mM Galur, 1.26 mM O_2 and 0.045 mM Cr^{VI} , in 2.0 M HClO_4 , at $T = 20^\circ\text{C}$. Spectra recorded every 3 min over a period of 20 min.

from the absorbance data obtained at 350 nm, and then confirmed for a number of $[\text{Galur}]$ and $[\text{H}^+]$, at 420–440 nm. The decrease in absorbance with time was not monophasic. Since it is known that Cr^{V} and Cr^{IV} species absorb at 350 nm and may, therefore, superimpose on the Cr^{VI} absorbance, Cr^{V} and Cr^{IV} contributions have to be taken into account when interpreting absorbance decay values, especially when the Cr^{VI} , Cr^{IV} and Cr^{V} decay rates are similar.⁴¹

In the redox reaction between Cr^{VI} and Galur relatively long-lived Cr^{V} species were observed in the EPR spectra, and CrO_2^{2+} , which can be taken as evidence that Cr^{IV} is involved in the reaction pathway, was also detected. Therefore, the kinetic profiles for the Galur/ Cr^{VI} system were fitted on the basis of the formation of Cr^{IV} and Cr^{V} intermediate species and the reaction could be adequately described by the set of first-order reactions shown in Scheme 2.



Scheme 2 $\text{Cr}^{\text{VI}} \rightarrow \text{Cr}^{\text{III}}$ reduction pathway used to fit the experimental absorbance data; I = very reactive intermediate.

Thus, taking into account the superimposition of Cr^{VI} , Cr^{IV} and Cr^{V} absorptions, the absorbance at 350 nm, at any time during the reaction, is given by:

$$A^{350} = \varepsilon^{\text{VI}}[\text{Cr}^{\text{VI}}] + \varepsilon^{\text{IV}}[\text{Cr}^{\text{IV}}] + \varepsilon^{\text{V}}[\text{Cr}^{\text{V}}] \quad (1)$$

Combining eqn. (1) with rate expressions⁴² derived from Scheme 2, we get:

$$A^{350} = A_0 e^{-2k_6 t} + k_6 \varepsilon^{\text{IV}} [\text{Cr}^{\text{VI}}]_0 (e^{-k_4 t} - e^{-2k_6 t}) / (2k_6 - k_4) + k_6 k_4 [\text{Cr}^{\text{VI}}]_0 \varepsilon^{\text{V}} [(e^{-k_5 t} - e^{-2k_6 t}) / (2k_6 - k_5) + (e^{-k_5 t} - e^{-k_4 t}) / (k_5 - k_4)] / (k_4 - 2k_6) \quad (2)$$

In this equation, ε^{IV} and ε^{V} refer to the molar absorptivity at 350 nm of the intermediate Cr^{IV} and Cr^{V} species. The complete set of data could be fitted with $\varepsilon^{\text{IV}} = 2300 \text{ M}^{-1} \text{ cm}^{-1}$ and $\varepsilon^{\text{V}} = 1800 \text{ M}^{-1} \text{ cm}^{-1}$ (at all $[\text{H}^+]$), which are consistent with reported values for Cr^{IV} and Cr^{V} species, with the metal bound to O-donor ligands.^{2,43,44} Parameters k_6 , k_4 and k_5 refer to the rate of disappearance of Cr^{VI} , Cr^{IV} and Cr^{V} , respectively, and were evaluated from a non-linear iterative computer fit of eqn. (2).⁴⁵ A typical fit of experimental data at 350 nm is shown in Fig. 5(a).

In order to verify the first-order dependence of rate upon Cr^{VI} , Cr^{IV} and Cr^{V} , the rate constants were calculated for various $[\text{Cr}^{\text{VI}}]_0$ at constant temperature, $[\text{Galur}]$, $[\text{H}^+]$ and ionic strength. As expected, k_6 , k_4 and k_5 were found to be essentially constant with increasing $[\text{Cr}^{\text{VI}}]_0$.

Table 1 summarizes values of k_6 , k_4 and k_5 for various concentrations of Galur at fixed concentrations of HClO_4 . Plots of k_6 vs. $[\text{Galur}]$ at constant $[\text{H}^+]$ show saturation kinetics (Fig. 6) from which values of K and k_{6h} were determined. K ($2.2 \pm 0.7 \text{ M}^{-1}$) is independent of $[\text{H}^+]$, whereas k_{6h} shows a second-order dependence on $[\text{H}^+]$ given by eqn. (3) (Fig. 6, inset):

Table 1 Observed pseudo-first-order rate constants (k_6 , k_5 , k_4) for different $[\text{HClO}_4]$ and $[\text{Galur}]^a$

$[\text{HClO}_4]/\text{M}$	0.20	0.40	0.63	0.80	0.97
$10[\text{Galur}]/\text{M}$	$10^3 k_6^b/\text{s}^{-1}$				
0.48	0.12(1)	0.32(1)	0.66(6)	1.4(1)	2.0(1)
0.96	0.27(1)	0.68(4)	1.4(1)	2.8(1)	4.2(2)
1.44	0.42(2)	1.0(1)	2.0(1)	4.2(2)	6.1(1)
1.92	0.60(2)	1.3(1)	2.3(1)	5.1(1)	7.1(3)
2.40	0.77(3)	1.3(1)	2.4(2)	5.8(3)	8.5(2)
	$10^3 k_5^b/\text{s}^{-1}$				
0.48	0.53(3)	0.67(6)	0.82(5)	1.0(4)	1.3(1)
0.96	0.70(7)	0.92(8)	1.3(1)	1.7(1)	1.9(1)
1.44	0.89(3)	1.2(1)	1.7(1)	2.4(1)	2.8(1)
1.92	1.1(1)	1.4(1)	2.1(1)	3.0(1)	3.5(1)
2.40	1.3(1)	1.7(1)	2.6(2)	3.5(1)	4.6(2)
	$10^3 k_4^b/\text{s}^{-1}$				
0.48	0.34(1)	0.54(4)	0.96(5)	1.6(1)	1.8(1)
0.96	0.58(5)	1.2(1)	2.3(1)	4.0(3)	6.7(3)
1.44	1.0(1)	2.5(2)	4.5(2)	8.1(4)	13(1)
1.92	1.2(1)	3.7(2)	8.1(3)	15(1)	21(1)
2.40	1.6(1)	5.3(6)	12(1)	21(1)	33(2)

^a $T = 33^\circ\text{C}$; $[\text{Cr}^{\text{VI}}]_0 = 6 \times 10^{-4} \text{ M}$; $I = 1.0 \text{ M}$. ^b Mean values from multiple determinations. Uncertainty in the last figure is given in parentheses.

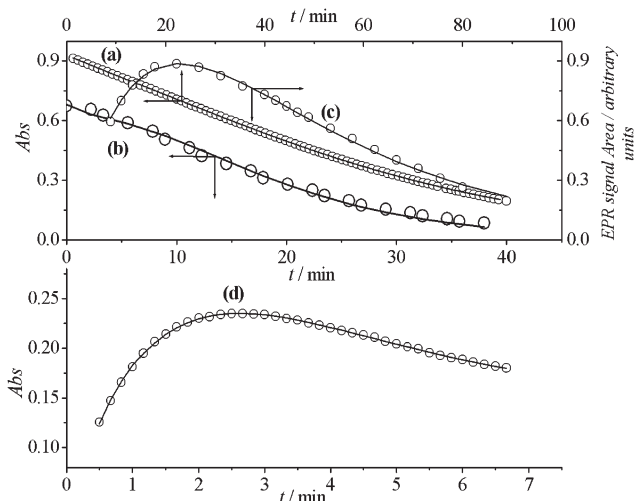


Fig. 5 Curves showing absorbance and EPR signal area vs. time for the oxidation of Galur by Cr^{VI} , $I = 1.0 \text{ M}$. (a) $\lambda = 350 \text{ nm}$, $[\text{Cr}^{\text{VI}}] = 6 \times 10^{-4} \text{ M}$, $[\text{Galur}] = 3.0 \times 10^{-2} \text{ M}$, $[\text{H}^+] = 0.63 \text{ M}$; $T = 33^\circ\text{C}$; (b) $\lambda = 440 \text{ nm}$, $[\text{Cr}^{\text{VI}}] = 3.0 \times 10^{-3} \text{ M}$, $[\text{Galur}] = 2.4 \times 10^{-1} \text{ M}$, $[\text{H}^+] = 0.40 \text{ M}$, $T = 33^\circ\text{C}$; (c) $g_{\text{iso}} = 1.9785$, $[\text{Cr}^{\text{VI}}] = 3.0 \times 10^{-2} \text{ M}$, $[\text{Galur}] = 0.83 \text{ M}$, $[\text{H}^+] = 0.10 \text{ M}$, $T = 20^\circ\text{C}$; (d) $\lambda = 570 \text{ nm}$, $[\text{Cr}^{\text{VI}}] = 8.0 \times 10^{-3} \text{ M}$, $[\text{Galur}] = 0.94 \text{ M}$, $[\text{H}^+] = 0.63 \text{ M}$, $T = 33^\circ\text{C}$. Fitted lines were calculated using eqns. (2), (9) and (11).

$$k_{6h} = k_{61} [\text{H}^+]^2 \quad (3)$$

with $k_{61} = (2.5 \pm 0.2) \times 10^{-2} \text{ M}^{-2} \text{ s}^{-1}$. Consequently, the rate constant for the Cr^{VI} consumption is expressed as:

$$k_6 = k_{61} [\text{H}^+]^2 [\text{Galur}] / ([\text{Galur}] + 1/K) \quad (4)$$

At constant $[\text{H}^+]$, k_4 showed quadratic dependence on $[\text{Galur}]$ (Fig. 7) whilst k_5 gave straight lines with positive intercept (Fig. 8), described by eqns. (5) and (6), respectively:

$$k_4 = k_{4h0} + k_{4h2} [\text{Galur}]^2 \quad (5)$$

$$k_5 = k_{5h0} + k_{5h2} [\text{Galur}] \quad (6)$$

The parameters k_{4h0} ($(4 \pm 2) \times 10^{-4} \text{ s}^{-1}$) and k_{5h0} ($(4 \pm 1) \times 10^{-4} \text{ s}^{-1}$) are independent of $[\text{H}^+]$. Plots of k_{4h2} and k_{5h2} vs. $[\text{H}^+]$ are shown in

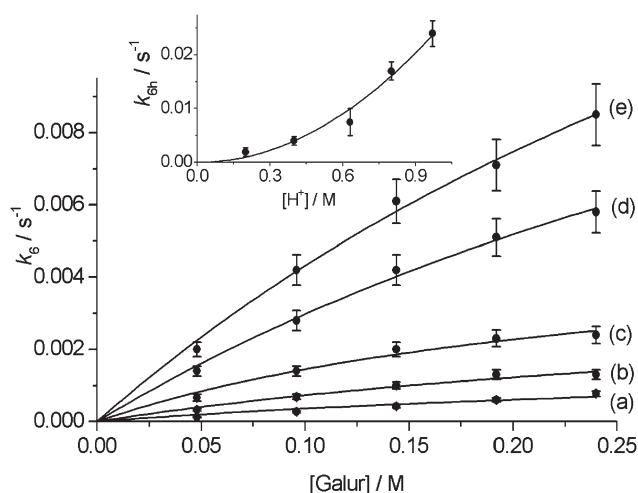


Fig. 6 Effect of [Galur] on k_6 at 33 °C, $I = 1.0$ M and $[H^+]$: (a) 0.20; (b) 0.40; (c) 0.63; (d) 0.80 and (e) 0.97 M. Inset: Quadratic dependence of k_{6h} on $[H^+]$.

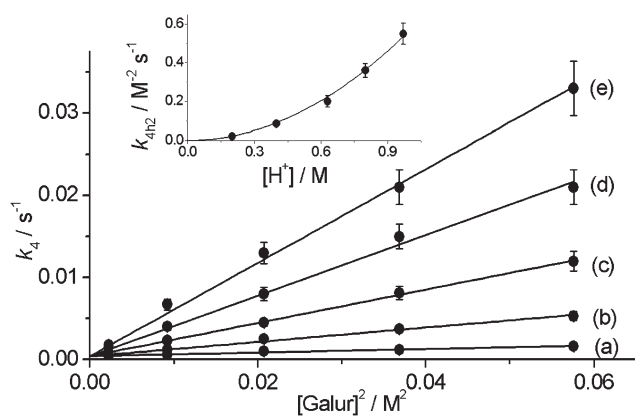


Fig. 7 Effect of [Galur] on k_4 at 33 °C, $I = 1.0$ M and $[H^+]$: (a) 0.20; (b) 0.40; (c) 0.63; (d) 0.80 and (e) 0.97 M. Inset: Effect of acidity on k_{4h2} .

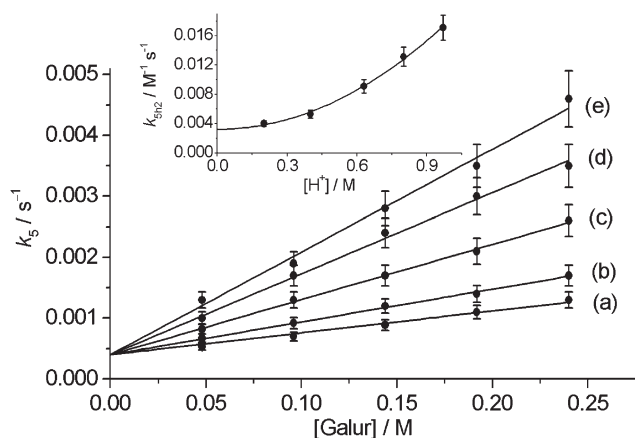


Fig. 8 (a) Effect of [Galur] on k_5 at 33 °C, $I = 1.0$ M and $[H^+]$: (i) 0.20; (ii) 0.40; (iii) 0.63; (iv) 0.80 and (v) 0.97 M. Inset: Effect of acidity on k_{5h2} .

the inset of Fig. 7 and 8, and the dependence of these rate constants on $[H^+]$ is given by eqns. (7) and (8):

$$k_{4h2} = k_{42}[H^+]^2 \quad (7)$$

$$k_{5h2} = k_{51} + k_{52}[H^+]^2 \quad (8)$$

with $k_{42} = (5.7 \pm 0.1) \times 10^{-1} \text{ M}^{-4} \text{ s}^{-1}$, $k_{51} = (3.2 \pm 0.2) \times 10^{-3} \text{ M}^{-1} \text{ s}^{-1}$, $k_{52} = (1.5 \pm 0.1) \times 10^{-2} \text{ M}^{-3} \text{ s}^{-1}$.

The values of k_6 , k_4 and k_5 obtained at 350 nm were used to simulate the kinetic traces at 420–440 nm and several $[H^+]$, and excellent fits to the experimental data were obtained using eqn. (2) (Fig 5(b)).

The values of k_6 , k_4 and k_5 and their dependencies with $[H^+]$ and $[Galur]$ were independently confirmed by following the redox reaction by EPR spectroscopy. The growth and decay of the Cr^V EPR signal was monitored in 0.025–0.50 M $HClO_4$, with higher modulation amplitude (4 G) and $[Cr^{VI}]_0$ than those used in the qualitative experiments described above (Fig. 5(c)). The higher values were required in order to obtain good intensity/noise ratios and hence accurate measurements of signal areas. The EPR data could be fitted to the expression (eqn. (9)) derived from Scheme 2 for the total Cr^V present in the mixture at any time.

$$A_{EPR} = k_6 k_4 [Cr^{VI}]_0 U [(e^{-k_5 t} - e^{-2k_6 t}) / (2k_6 - k_5) + (e^{-k_5 t} - e^{-k_4 t}) / (k_5 - k_4)] / (k_4 - 2k_6) \quad (9)$$

where the parameter U depends on the EPR spectrometer acquisition conditions (gain, power, modulation, etc.). When the substrate to Cr^{VI} ratio was higher than 30:1, the values at 20 °C of k_6 , k_4 and k_5 calculated by eqn. (9) were the same (within the experimental error) as those obtained from the spectrophotometric data, using eqn. (2) or calculated from eqns. (4)–(8) corrected for the temperature change. Even at pH 1.61, the kinetic profiles could be fitted by eqn. (9), for Galur: Cr^{VI} ratios >30:1. When the Galur: Cr^{VI} ratio was <20:1, the rate constants deviated from the expected values. A probable explanation is that, when there is only a small excess of Galur over Cr^{VI} , the concentration of Galur in the reaction mixture approaches or exceeds that of Galur as the reaction proceeds, thus competing with Galur for reaction with Cr^{VI} . This results in overall rate constants that are different from those obtained with a large excess of Galur, when to a good approximation it is the only active reductant in the mixture.

The electronic and EPR spectra show that the final Cr species in the reaction mixture is Cr^{III} . However, kinetic traces at 570 nm indicate that at this wavelength, the absorbance grows to intensities higher than that expected for Cr^{III} and then decay to the value expected for Cr^{III} . The higher intensity of the Cr^{III} band may be due either to the presence of underlying absorption due to intermediate Cr^V (or Cr^{IV}) species or to the presence of an intermediate Cr^{III} complex, which then decomposes to the final product. For a set of experiments performed in 0.63 M $HClO_4$ and Galur: Cr^{VI} ratios of 60–120:1, the absorbance vs. time curves at 570 nm could be fitted adequately if the absorption of a Cr^V intermediate species was considered besides that of Cr^{III} . Thus, the total absorbance at 570 nm (A_{570}) at any time is given by eqn. (10).

$$A_{570} = \epsilon^V [Cr^V] + \epsilon^{III} [Cr^{III}] \quad (10)$$

Combining eqn. (10) with rate expressions derived from Scheme 2 for $[Cr^V]$ and $[Cr^{III}]$ present in the reaction mixture, we get:

$$A_{570} = \epsilon^{III} [Cr^{VI}]_0 \left\{ [1 - e^{-2k_6 t} - k_6 (e^{-2k_6 t} - e^{-k_4 t})] / (k_4 - 2k_6) + (\epsilon^V - \epsilon^{III}) k_6 k_4 [Cr^{VI}]_0 [(e^{-2k_6 t} - e^{-k_5 t}) / (k_5 - 2k_6) - (e^{-k_4 t} - e^{-k_5 t}) / (k_5 - k_4)] \right\} / (k_4 - 2k_6) \quad (11)$$

The best fits of experimental data were obtained with $\epsilon^V = 79 \text{ M}^{-1} \text{ cm}^{-1}$ and $\epsilon^{III} = 21 \text{ M}^{-1} \text{ cm}^{-1}$,^{2,44} and a typical fit is shown in Fig. 5(d). Values of k_6 , k_4 and k_5 calculated at this wavelength are consistent with those obtained by using either eqns. (2) or (9). These results indicate that the intermediate Cr^V species should be responsible for the growth and decay of the absorbance at 570 nm. Besides, the kinetics profiles simulated with the parameters calculated by either eqns. (2), (9) or (11) show that the time of maximum intensity (t_{max}) of the A_{570} is very close to the time calculated for $[Cr^V]_{max}$ in the reaction mixture (up to 25% of the total chromium in the solution) and is coincident with the experimental t_{max} observed by EPR under the same reaction conditions.

Discussion

Characterization of Cr^V -Galur species

EPR spectroscopy is the most sensitive method for characterising Cr^V complexes in solution. The values of the spectral parameters, g_{iso} and A_{iso} , together with the any proton shfs, are useful for de-

termining the nature of the bonding of the sugar molecules to the Cr^V centre.^{2,14,46–48} An empirical relationship between the nature and number of donor groups and the EPR spectral parameters of Cr^V complexes has been established,^{2,47} and five-coordinated Cr^V species have higher g_{iso} and lower $^{53}\text{Cr } A_{\text{iso}}$ values than the corresponding six-coordinated species.^{32,47,49} Assignment of the structures of the new oxo–Cr^V(Galur) species in the solutions in the present experiments have, therefore, been made on the basis of the isotropic EPR parameters (g_{iso} and A_{iso} values) and the proton shfs from the ligand.^{2,47}

It is known that the five-membered Cr^V chelates are favoured^{31,50,51} and, in addition, Galur is well suited for stabilization of five-membered Cr^V chelates since it possesses 2-hydroxycarboxylate and *vic*-diolato sites for potential chelation.

For the reaction of Cr^{VI} with Galur, at any [H⁺] between 1.0 M HClO₄ and pH 5, and ligand to metal ratios $\geq 20:1$ (Fig. 1(b)), the EPR spectra of the intermediate Cr^V species consist of two triplets with $g_{\text{iso}1} = 1.9786$ and $g_{\text{iso}2} = 1.9784$ and one doublet with $g_{\text{iso}3} = 1.9785$; the $^{53}\text{Cr } A_{\text{iso}} = 17.2(1) \times 10^{-4} \text{ cm}^{-1}$ for each species. The g_{iso} and A_{iso} values correspond to those calculated for five-coordinated oxo–Cr^V complexes with two carboxylate and two alcoholato donor groups.⁴⁷

The shfs of the signals with $g_{\text{iso}1}$ and $g_{\text{iso}2}$ is that expected for two equivalent carbinolic protons coupled to the Cr^V electronic spin. In order to yield the most favoured five-membered Cr^V chelates, these carbinolic protons must belong to the α -hydroxycarboxylate donor site of two bidentate Galur molecules bound to Cr^V, giving $[\text{Cr}^{\text{VO}}(\text{O}^6, \text{O}^5\text{-galactofuranuronate})_2]^-$. The formation of such a Cr^V bischelate is only possible with Galur bound to Cr^V in the furanose form. However, in the pH range 2–8, Galur exists in aqueous solution as an equilibrium between the pyranose and furanose isomers, in about 9:1 ratio, with the β -anomer being the most stable one.⁵² Thus, the furanose form which is the less stable in aqueous solution is the one preferred in complexation. This finding is similar to that found in NMR studies of MoO₄²⁻ and WO₄²⁻–Galur systems where the pronounced high frequency shifts for the nuclei at positions 5 and 6 provided evidence for complexation involving the carboxylate and the adjacent carbinol group as the major species in solution.^{52,53} The different shfs constants for the two triplets indicate that they correspond to the two geometric isomers of the Cr^V bischelate $[\text{Cr}(\text{O})(\text{O}^5, \text{O}^6\text{-galactofuranuronate})_2]^-$ (I and II in Fig. 9).

The doublet shfs for the species with $g_{\text{iso}3}$ indicates that, in this oxo–Cr^V(Galur)₂ complex, only one carbinolic proton is coupled to the Cr^V electronic spin. This can be assigned to the Cr^V bischelate

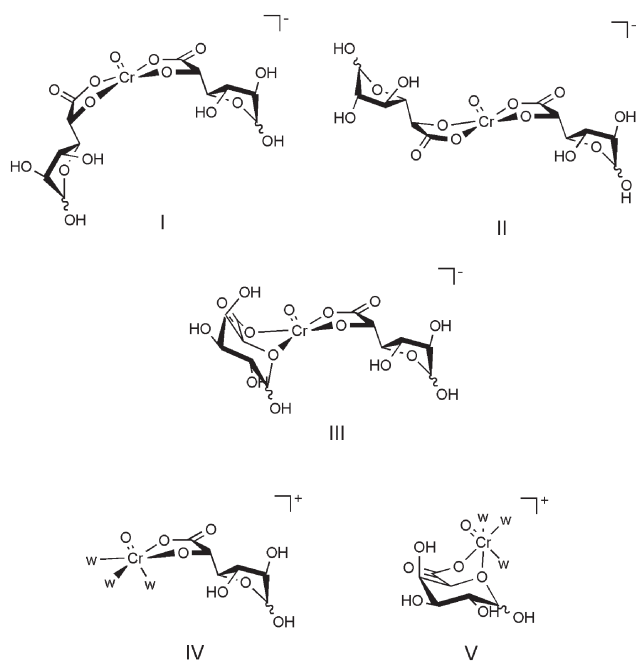


Fig. 9 Structures of Cr^V complexes with Galur.

$[\text{Cr}(\text{O})(\text{O}^{\text{ring}}, \text{O}^6\text{-galactopyranuronate})(\text{O}^5, \text{O}^6\text{-galactofuranuronate})]^-$ (III), with one Galur molecule acting as a bidentate ligand through the α -hydroxycarboxylate moiety of the furanose form and the second bound to the Cr^V at the carboxylate group and the ring oxygen of the pyranose form. This kind of coordination for the pyranose form of Galur has also been proposed as an explanation for a minor species in its complexation of MoO₄²⁻.⁵³

Assignment of the EPR signals to Cr^V monochelates was ruled out on the basis of the effect of the ligand concentration on the signal at constant pH. The independence of the spectra on [Galur] confirms that all the three species have a Cr^V coordination sphere saturated with respect to the alduronic acid (*i.e.* Cr^V(Galur)₂).

The fact that the EPR spectra are composed of the same three species when either very large (1200–7000:1) Galur to Cr^{VI} ratios are used or upon addition of Galur to an equimolar glutathione–Cr^{VI} mixture, eliminates the possibility of one of the three Cr^V species being formed by chelation to the oxidation product. This was also confirmed by experiments where Cr^V was generated by reaction of glutathione with Cr^{VI} and then stabilised by addition of Galur at pH 4.5. This reaction mixture yielded two triplets with $g_{\text{iso}} = 1.9780$ and 1.9785, corresponding to the two geometric isomers of $[\text{Cr}^{\text{VO}}(\text{O}^1, \text{O}^2\text{-Galur})]^-$, with g_{iso} and/or shfs different from those observed for the Cr^{VI}–Galur system.

In 0.5 and 0.75 M HClO₄ and 10:1 ligand:Cr^{VI} ratio, ($[\text{Cr}^{\text{VI}}]_0 = 2 \text{ mM}$), one additional signal with $g_{\text{iso}} = 1.972$ appeared along with the signal centred at $g_{\text{iso}} = 1.9785$. Although the shfs of this new signal was not resolved, its g_{iso} value and the dependence of its intensity on pH, [Galur]:[Cr^{VI}] ratio and $[\text{Cr}^{\text{VI}}]_0$ affords some information on its nature. First, the low g_{iso} value suggests a six-coordinated oxo–Cr^V species, possibly $[\text{Cr}(\text{O})(\text{O}^5, \text{O}^6\text{-Galur})(\text{H}_2\text{O})_3]^+$ (IV) or $[\text{Cr}(\text{O})(\text{O}^{\text{ring}}, \text{O}^6\text{-Galur})(\text{H}_2\text{O})_3]^+$ (V), since the calculated g_{iso} value for a six-coordinated oxo–Cr^V species with one 2-hydroxycarboxylate donor and three water molecules (1.971) is in reasonable agreement with the observed g_{iso} value. Furthermore, the fact that the signal was observed at low [Galur] to [Cr^{VI}] ratio favours its assignment to an oxo–Cr^V monochelate, whilst the positive charge is consistent with its appearance at high [H⁺].

For the reaction of excess of Galur with Cr^{VI} at pH 7.5, the Cr^V EPR signal appears at $g_{\text{iso}} = 1.9793$, a value higher than observed at lower pH. This g_{iso} value corresponds to those calculated for five-coordinated oxo–Cr^V complexes with four alcoholato donor groups.⁴⁷ It is known that, at this pH, α -hydroxy acids are not able to stabilise Cr^V toward disproportionation, whereas linear *vic*-diols or cyclic *cis*-diols produce Cr^Vdiolate₂ complexes that are more stable in solution.^{2,46} As expected, at pH 7.5, lactic acid, an α -hydroxy acid with no *vic*-diolato groups, did not produce any Cr^V–lactic acid EPR signal when it was added to a glutathione–Cr^{VI} mixture. Several molecules possessing both the *vic*-diol (or cyclic *cis*-diol) and 2-hydroxycarboxylate groups yield exclusively the Cr^V(diolate)₂ complexes at pH 7.5, whilst the Cr^V(2-hydroxycarboxylate)₂ chelates are the major species formed at pH ≤ 5 . The shift of the Cr^V–Galur EPR signal toward higher g_{iso} values at pH 7.5 implies the formation of a Cr^V complex where the *vic*-diol groups of Galur participates in the bonding to Cr^V. Given the marked preference of the CrO³⁺ ion for binding to *cis*- rather than *trans*-diolato groups of cyclic diols, the Cr^V species formed at pH 7.5 in the reaction of Galur with Cr^{VI} can be assigned to $[\text{Cr}(\text{O})(\text{cis-} \text{O}^3, \text{O}^4\text{-galactopyranuronate})_2]^-$.¹⁴ Similar behaviour was observed with the galactonic acid (Gala)–Cr^V and Cr^V–quinic acid systems, where at pH 7.5, Cr^V bonding to the cyclic-*cis*-diolato groups is preferred.^{27,50}

The lack of chelation at any *vic*-diolate group of Galur when pH ≤ 5 , differentiates its ability to stabilise Cr^V from that of galactose¹⁹ and its derivatives: methyl galactopyranoside,¹⁴ lactose and melibiose,¹⁵ all molecules that have been found to form oxo–Cr^V(diolate)₂ species $[\text{Cr}(\text{O})(\text{cis-} \text{O}, \text{O}\text{-saccharide})_2]^-$ ($g_{\text{iso}} \approx 1.9800\text{--}1.9795$ and $A_{\text{iso}} \approx 16.5 \times 10^{-4} \text{ cm}^{-1}$) at any pH. The $[\text{Cr}(\text{O})(\text{cis-} \text{O}, \text{O}\text{-saccharide})_2]^-$ species are extremely stable and at pH 3–5 remain in solution for several months, whereas in this pH range, the Galur–Cr^V species grow and decay over much shorter periods, similar to those of $[\text{Cr}(\text{O})(\alpha\text{-hydroxy acid})_2]^-$.¹⁰

The reduction of Cr^{VI} by Galur is strongly dependent on pH. Although the reaction is slow at pH > 1, Cr^{VI} is rapidly consumed when the [H⁺] > 0.1 M. For this reason, the 0.2–1.0 M [H⁺] range was chosen to study the kinetics of this reaction. The time-dependent UV/vis spectra of the reaction mixture show that the absorbance at 350 nm and 420–470 nm decays with time, while absorbance at 570 nm increases, without an isosbestic point (Fig. 10). The lack of an isosbestic point indicates that there are two or more competing reactions at any time and that in the reduction of Cr^{VI} to Cr^{III} intermediate chromium species are present in appreciable concentrations.

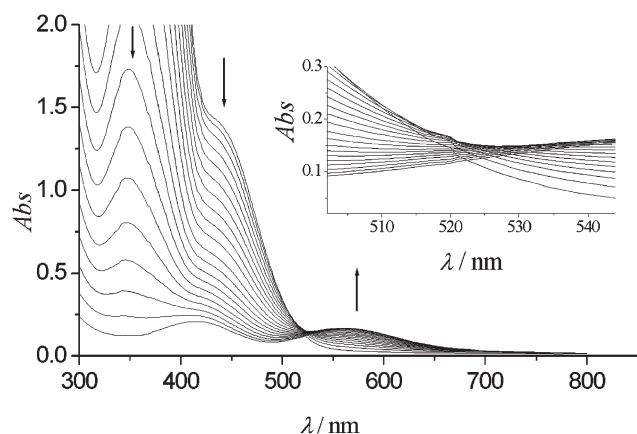


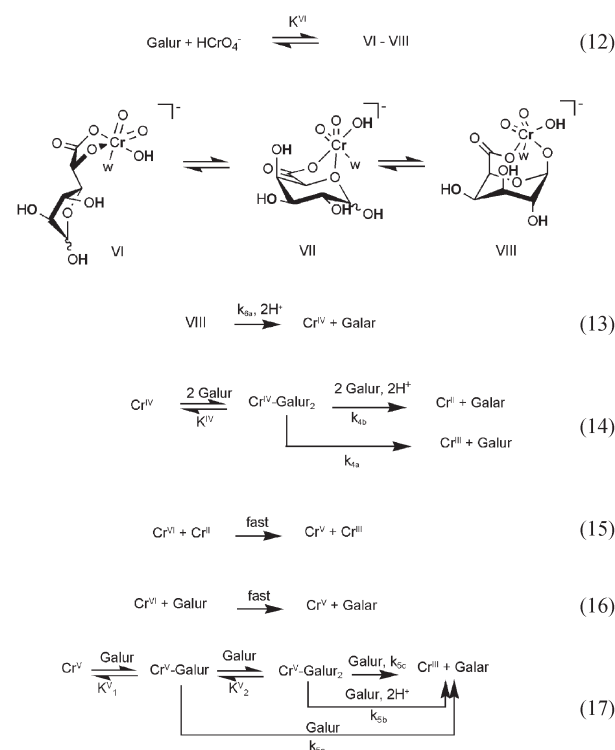
Fig. 10 Time evolution of the UV/vis spectra from a mixture of Galur (0.30 M) and Cr^{VI} (6.0×10^{-3} M) over a period of 1 h; [HClO₄] = 0.20 M; $T = 33$ °C. Spectra recorded every 2 min; first spectrum taken 11 min after the reaction started.

Thus, the kinetic traces demonstrate that the reduction of Cr^{VI} by Galur is more complex than the reaction with neutral monosaccharides and glycosides.^{14,15} The kinetic data for reactions of Cr^{VI} with aldoses,¹⁴ alditols,⁵⁴ aldonic acids^{27,29} and methyl glycosides¹⁵ could be fitted with two consecutive first-order steps, but with Galur, the presence of two different chromium intermediates is required to fit the experimental data. These two intermediates have absorbance extinction coefficients similar to those of characterised Cr^{IV} and Cr^V compounds.^{2,10,44,55} Formation of Cr^V and/or Cr^{IV} intermediates by the redox reaction of Cr^{VI} with the substrate has been observed previously for a number of substrates.^{2,11,56,57} The fact that CrO₂²⁺ is detected in the reaction of Galur with Cr^{VI} together with the observation of relatively long lived Cr^V species in the EPR experiments, indicate that both Cr^{IV} and Cr^V intermediate species are formed in this reaction. Therefore, the time dependence of the reaction absorption data at several wavelengths can be fitted with the sequence proposed in Scheme 2. Besides, the curves for EPR area vs. time can be fitted with eqn. (9) and the first-order rate constants obtained from these measurements, for Galur:Cr^{VI} ratios >30:1, in 0.025–0.5 M HClO₄, agree perfectly with those calculated from the electronic spectroscopy data.

By taking account of (a) the kinetic results, (b) the polymerisation of acrylonitrile added to the reaction mixture, (c) the detection of an intermediate Cr^{VI} ester at high pH, (d) the detection of Cr^V species by EPR, (e) the absence of an isosbestic point, (f) the observation of CrO₂²⁺, and (g) the formation of Galar as the only organic reaction product, we are now able to propose a possible mechanism for the reaction of Galur with Cr^{VI}. This is presented in the following paragraphs.

At the [H⁺] and [Cr^{VI}] used in the kinetics studies, Cr^{VI} exists as HCrO₄⁻;⁵⁸ it is proposed that this species is the reactive form of Cr^{VI}, which is also in agreement with the first-order dependence of the reaction rate on [Cr^{VI}]. The oxidation of alcohols by Cr^{VI} is preceded by the formation of a chromate ester.^{34,41} The observation of the absorbance bands characteristic of chromate oxy-esters around 360 and 387 nm 2 min after mixing Galur and Cr^{VI} under conditions where the redox reaction is slow, indicates that at least two

intermediate Cr^{VI} complexes are formed rapidly prior to the redox steps. Thus, the first step of the mechanism proposed in Scheme 3 is the formation of the Galur–Cr^{VI} monochelates **VI–VIII**, which is also consistent with the saturation kinetics observed for k_6 with [Galur]. Several coordination modes are possible for the Cr^{VI}–Galur species, but the complex with the anomeric hydroxyl group bound to Cr^{VI} (**VIII**) is the only redox active intermediate, since the oxidation of Galur occurs only at this position. Complex **VIII** must also be in rapid equilibrium with any other linkage isomer (**VI**, **VII**) because the absorbance bands around 360 and 387 nm from the esters decay with the same rate. The slow step proposed in Scheme 3 for the Cr^{VI} consumption involves the intramolecular two-electron transfer within the active Cr^{VI}–Galur species (**VIII**) to yield Cr^{IV} and Galar (eqn. (13)). The conversion of intermediate **VIII** into Cr^V and Galar requires two protons, so that the redox reaction should be favoured in acid medium, such as observed. The rate law for the Cr^{VI} consumption derived from eqns. (12) and (13) in Scheme 3 is given by eqn. (18), where [Cr^{VI}]_T refers to the total [Cr^{VI}] in the reaction mixture.



Scheme 3 Proposed mechanism of the Galur oxidation by Cr^{VI} in acidic media; w = OH₂.

$$-d[\text{Cr}^{\text{VI}}]/dt = k_{6a}K^{\text{VI}}[\text{H}^+]^2[\text{Galur}][\text{Cr}^{\text{VI}}]_{\text{T}}/(1 + K^{\text{VI}}[\text{Galur}]) \quad (18)$$

Eqn. (18) agrees perfectly with the experimental rate law (eqns. (3) and (4)).

The kinetic data indicate that Cr^{IV} formed in eqn. (13) can further oxidize Galur through two competitive slow steps to yield the redox products. The ϵ^{IV} determined from the fit of the experimental absorption data suggests the formation of a Cr^{IV}(Galur)₂ bischelate.⁴⁴ Therefore, in the scheme, it is proposed that Cr^{IV} reacts with Galur to form a Cr^{IV}(Galur)₂ bischelate (K^{IV}), which can yield the redox products directly (k_{4a}) or in the presence of additional Galur through an acid catalysed step (k_{4b}). Two different redox products are proposed to form through the two parallel steps of eqn. (14): Cr^{III} and the Galur[•] radical or Cr^{II} and Galar. The first is supported by the observed polymerisation of acrylonitrile when it is added to the reaction mixture, while the second, by the formation of CrO₂²⁺, the product of the reaction of Cr^{II} with O₂, which is taken as evidence of the Cr^{IV} formation.^{35,36} If Cr^{IV}(Galur)₂ is considered to be the major Cr^{IV} species present in the mixture, the rate law for the disappearance of Cr^{IV} takes the form of eqn. (19), which is in total agreement with the experimental rate law (eqns. (5) and (7)):

$$-d[\text{Cr}^{\text{IV}}]/dt = \{k_{\text{a}} + k_{\text{b}}[\text{H}^+]^2[\text{Galur}]^2\}[\text{Cr}^{\text{VI}}]_{\text{T}} \quad (19)$$

Cr^{V} can form by fast reaction of Cr^{II} with Cr^{VI} (eqn. (15)) – the $[\text{Cr}^{\text{VI}}]$ used in the kinetic experiments is higher than used for the detection of CrO_2^{2+} , therefore Cr^{VI} can successfully compete with O_2 for Cr^{II} – and, alternatively, by rapid reaction of the Galur \cdot radical with Cr^{VI} (eqn. (16)). The reaction of Galur \cdot with Cr^{VI} should be very fast and prevents the detection of the organic radical in the EPR measurements. The kinetic data indicate that Cr^{V} formed in the fast steps can further oxidize Galur through three competitive slow steps to yield Cr^{III} and Galar as the final redox products. Therefore, on the basis of the EPR and kinetics results, in Scheme 3, it is proposed that Cr^{V} reacts with Galur to form an oxo- Cr^{V} (Galur) monochelate (K^{V}_1) in rapid equilibrium with the oxo- Cr^{V} (Galur) $_2$ bischelate (K^{V}_2). These Cr^{V} intermediates yield the redox products in the presence of another Galur molecule, directly (k_{sa} and k_{sc}) or through an acid catalysed step (k_{sb}). The Cr^{V} (Galur) and Cr^{V} (Galur) $_2$ complexes in eqn. (17) represent several linkage isomers – the structure of the major ones (I–V) was discussed above – but the selectivity of the oxidation of Galur requires that the complex with the anomeric hydroxyl group bound to Cr^{V} should be the redox active Cr^{V} species. The fact that Galur is oxidised at a higher rate than any of the aldoses (either pyranoses or furanoses), which are also oxidised at the hemiacetalic position but form stable oxo- Cr^{V} (diolate) $_2$ species at $\text{pH} > 1$, suggests that the redox active Cr^{V} species could be of the type $[\text{Cr}^{\text{V}}(\text{O})(\text{O}^1, \text{O}^6\text{-Galur})(\text{O}^6, \text{O}^5\text{-Galur})]^-$, with C1–O and the carboxylate bound to Cr^{V} . If Cr^{V} (Galur) $_2$ bischelates are considered to be the major Cr^{V} species present in the mixture, oxo- Cr^{V} bischelates are the major Cr^{V} species observed by EPR spectroscopy for Galur : Cr^{VI} ratios $>30:1$ at $\text{pH} \leq 5$, and oxo- Cr^{V} (Galur) monochelates are only observed as minor species when the Galur : Cr^{VI} ratio ≤ 10 and $[\text{H}^+] > 0.25 \text{ M}$, the rate law for the disappearance of Cr^{V} takes the form of eqn. (20), which is in total agreement with the experimental rate law (eqns. (6) and (8)):

$$-d[\text{Cr}^{\text{V}}]/dt = \{k_{\text{sa}}/K^{\text{V}}_2 + (k_{\text{sb}}[\text{H}^+]^2 + k_{\text{sc}})[\text{Galur}]\}[\text{Cr}^{\text{V}}]_{\text{T}} \quad (20)$$

The first term in the rate law represents the relative redox vs. substitution rate of the (Galur) Cr^{V} monochelate. From eqn. (6) the value of $k_{\text{sa}}/K^{\text{V}}_2$ ($k_{\text{sb}0}$) is $4 \times 10^{-4} \text{ s}^{-1}$, meaning that the (Galur) Cr^{V} monochelate yields the redox products more than 10^3 -times slower than reacts with Galur to form the Cr^{V} (Galur) $_2$ bischelate. The excess of Galur over Cr^{V} in all the experiments also favours the bischelate formation. The redox reaction can still occur at low $[\text{H}^+]$, through the acid independent paths (k_{sa} and k_{sc}), such as observed in the EPR measurements.

Experimental

Materials

α -D-Galacturonic acid monohydrate (Sigma, 98%, mp 161–162 °C), galactaric acid (Sigma, 95.8%), lactic acid (Baker, 88% aqueous solution), L-(+)-tartaric acid (Sigma ultra, 99.5%), glutathione (reduced form, Sigma, 98–100%), potassium dichromate (Mallinckrodt), sodium chromate (Merck), $^{53}\text{Cr}_2\text{O}_3$ (Atomic Energy Research Establishment, Harwell, England, 95%), perchloric acid (A.C.S. Baker), acrylonitrile (Aldrich, 99%), acrylamide (Sigma, >99%), sodium hydroxide (Cicarelli, p.a.) were used without further purification. Water was deionised (purite Select Analyst HP, Thame Oxon, UK) or doubly distilled over KMnO_4 .

4-(2-Hydroxyethyl)-1-piperazineethanesulfonic acid (HEPES) buffer (Sigma ultra, >99.5%) was added to adjust the pH value of the solution to 7.5. Galactaric acid (Galar) solutions of pH 4–5 were obtained by dissolving Galar at pH 8 and then acidifying by slow addition of HClO_4 to the desired pH.

For experiments performed in the 1–5 pH range, the pH of the solutions was adjusted by addition of 0.5 M HClO_4 or 1.0 M NaOH . In experiments performed at constant ionic strength ($I = 1.0 \text{ M}$) and different hydrogen ion concentrations, mixtures of sodium perchlorate solutions and perchloric acid solutions were used. Sodium perchlorate solutions were prepared from sodium hydroxide and

perchloric acid solutions. The concentration of stock solutions of perchloric acid was determined by titration employing standard analytical methods.

CAUTION. Cr^{VI} compounds are human carcinogens, and Cr^{V} complexes are mutagenic and potential carcinogens.⁵⁹ Contact with skin and inhalation must be avoided. Acrylonitrile is a carcinogen and must be handled in a well-ventilated fume hood.⁶⁰

Methods

Product analysis. Under the conditions used in the kinetic measurements (excess of Galur over Cr^{VI}), Galar was identified as the only reaction product by HPLC. The chromatograms were obtained on a KNK-500 A chromatograph provided with a 7125 HPLC pump. The separation was carried out on a Supelcogel C-610H HPLC column ($300 \times 7.8 \text{ mm}$, Bio-Rad Laboratories) using 0.1% v/v H_3PO_4 as eluent and a flow rate of 0.4 mL min^{-1} , at 30 °C. The effluent was monitored with a UV detector (115 UV Gilson, $\lambda = 210 \text{ nm}$). The $[\text{H}^+]$ of the standard and the reaction mixture samples was adjusted to 0.1 M by addition of HClO_4 and the samples then filtered through a $0.2 \mu\text{m}$ membrane prior to the injection into the chromatographic system.

Standard solutions of Galur and Galar were prepared individually in 0.10 M HClO_4 and the chromatographic retention times determined separately. Two peaks at $t = 624$ and 753 s were detected in reaction mixtures containing 30- to 100-times excess of Galur over Cr^{VI} in 0.10 M HClO_4 , in addition to the peak from Galur at $t = 859 \text{ s}$. The retention times of these new peaks are coincident with those of a standard solution of Galar. Furthermore, co-chromatography of a Cr^{VI} + Galur reaction mixture with added Galar resulted in the increase of the peaks at 624 and 753 s. Reaction mixtures with Galur : Cr^{VI} ratios lower than 30 : 1 yielded more complex chromatograms because of further oxidation of Galur.

For the Galur to Cr^{VI} ratios used in the kinetic studies (higher than 30 : 1), neither carbon dioxide nor formic acid was detected as a reaction product.

Galacturonic acid stability. The stability of Galur under conditions used in the kinetic studies was checked by monitoring the optical rotation changes using the sodium D line on an JENA polarimeter with thermostated 20 cm tubes. Previously thermostated reactant solutions were transferred into the cell immediately after mixing and the optical rotation was recorded at different time intervals after the preparation of the solutions. The specific rotation found at different times $[\alpha]^{20}_{\text{D}} = +97.2 \pm 0.5$ ($c = 10 \text{ g}/100 \text{ mL}$, aqueous solution, $t = 5 \text{ min}$), $[\alpha]^{20}_{\text{D}} = +50.5 \pm 0.5$ ($c = 10 \text{ g}/100 \text{ mL}$, aqueous solution or 1.0 M HClO_4 , $t = 24 \text{ h}$) are consistent with literature values.⁶¹ Equilibrated α/β -D-galacturonic acid solutions were used in the kinetic measurements.

The stability of Galur was also monitored by HPLC. Chromatograms recorded after incubation of the standard sample in 2.0 M HClO_4 (higher than the highest $[\text{H}^+]$ used in the kinetic measurements) at 40 °C during 48 h, were identical to those of the freshly prepared sample.

Polymerisation test. Polymerisation of acrylonitrile was investigated during the reaction of Galur with Cr^{VI} as a test for free radical generation. In a typical experiment, 0.5 mL of acrylonitrile was added to a solution of $\text{K}_2\text{Cr}_2\text{O}_7$ (2.4 mg, $8 \times 10^{-3} \text{ mmol}$) and monohydrate Galur (25.5 mg, 0.12 mmol) in 3 mL of 0.63 M HClO_4 at 40 °C. After a few minutes, a white precipitate appeared. Control experiments (without $\text{K}_2\text{Cr}_2\text{O}_7$ or reductant present) did not produce the precipitate. Possible reactions of Cr^{V} and Cr^{IV} with acrylonitrile were tested with $[\text{Cr}^{\text{V}}\text{O}(\text{ehba})_2]$ and $[\text{Cr}^{\text{IV}}\text{O}(\text{ehbaH})_2]$.^{43,55} No precipitation occurred on mixing the Cr^{V} or Cr^{IV} complexes with acrylonitrile under the conditions used in the Cr^{VI} + Galur reaction.

Spectrophotometric measurements. Kinetic measurements were made by monitoring absorbance changes on a Jasco V-530 spectrophotometer with fully thermostated cell compartments. The

reactions were followed under pseudo-first-order conditions, using at least a 30-fold excess of Galur over Cr^{VI}. Reactant solutions were thermostated prior to the experiment and transferred into a cell of 1 cm path length immediately after mixing. Measurements were made at 33 °C unless stated otherwise.

Disappearance of Cr^{VI} was followed by monitoring the absorbance at 350 nm until at least 80% conversion. In most experiments the initial concentration of Cr^{VI} was 6×10^{-4} M whilst the Galur concentration was varied from 0.03 to 0.30 M. The observed rate constants (k_6 , k_4 and k_3), were deduced from multiple determinations and were within $\pm 10\%$ of each other. The rate constants obtained at 350 nm were used to fit the absorbance changes at 420–440 nm. The goodness of fits at these wavelengths were used to corroborate the rate expressions used to obtain the rate constants at 350 nm.

At the end of the reaction of 8.0×10^{-3} M Cr^{VI} with excess Galur in 0.20–1.00 M HClO₄ at 33 °C, two d–d bands at $\lambda_{\text{max}} = 415$ and 570 nm, attributable to the octahedral ${}^4A_{2g} \rightarrow {}^4T_{1g}$ and ${}^4A_{2g} \rightarrow {}^4T_{2g}$ transitions of Cr^{III} in O_h symmetry,⁶² were observed in the electronic absorption spectrum. The formation of Cr^{III} at 33 °C was monitored by following changes in the 570 nm absorption band. In these experiments, the [Cr^{VI}]₀ was kept constant at 8×10^{-3} M and the [Galur] was varied between 0.48 and 0.94 M, in 0.63 M HClO₄. Rate constants obtained at this wavelength are in agreement with those calculated from data at 350 nm for these experimental conditions.

The possible formation of Cr^{II} was examined by periodic scanning of solutions of Galur (0.114 M), Cr^{VI} (1.6×10^{-2} mM) and 0.40 M HClO₄ in air-saturated ([O₂] = 0.26 mM) and oxygen saturated ([O₂] = 1.26 mM) solutions. Under these conditions, the band at 350 nm decreased in intensity over a period of 20 min, while new bands at 290 and 249 nm appeared. The new bands were attributed to CrO₂²⁺, formed as a long-lived intermediate.

Chromate esters were investigated by UV/vis spectrophotometry in the 350–400 nm region in which they show characteristic absorption bands. Reactions were performed at pH 6.5 (HEPES buffer), a pH where the redox reaction is slow enough to enable the observation of the ester formation. The instrument was zeroed to an arrangement of the reference and sample beams passing through matched cuvettes, both containing 6×10^{-4} M Cr^{VI} at pH 6.5. The solution in the sample cell was replaced with the reaction solution containing 6×10^{-4} M Cr^{VI} and 0.03–0.06 M Galur at pH = 6.5, $I = 2.0$ M and $T = 27$ °C. Spectra obtained within 30 min after mixing revealed two distinct absorptions at 360 and 387 nm.

EPR measurements. The EPR spectra were obtained with a Bruker ESP 300 E computer controlled spectrometer operating at X-band frequencies (~9 GHz). Microwave generation was by means of a klystron (ER041MR) and frequencies were measured with a built-in frequency-counter. Spectra were recorded as first derivatives of the microwave absorption in 1024 points at ambient temperature (20 ± 1 °C) using 8 mW microwave power and 100 kHz modulation frequency. Various modulation amplitudes are indicated individually in the text. g -Values were determined by reference to diphenylpicrylhydrazyl (DPPH) ($g = 2.0036$) as an external standard.

All of the EPR spectra were simulated using the PEST WinSIM program⁶³ assuming 100% Lorentzian line shapes. The spectral parameters for each Cr^V species were similar in all simulations, with maximum deviations of ± 0.0001 in the g_{iso} values. Values for $a_{\text{iso}}(^1\text{H})$ were included in the simulations only when they were greater than the line width of the Cr^V species.

Acknowledgements

We thank the National Research Council of Argentina (CONICET), the Scottish Office Environment and Rural Affairs Department, the Third World Academy of Sciences (TWAS), the National University of Rosario (UNR), ANTORCHAS Foundation, the ALFA Program (CROCON Network, Project ALR/B7-940470064), and the International Foundation for Sciences (IFS) for financial support, and CONICET and CONICYT for a bilateral agreement (CH-PA/01-E04).

References

- 1 C. B. Klein, in *Toxicology of Metals*, ed. L. W. Chang, CRC-Lewis Publishers, New York, 1996, pp. 205–220.
- 2 R. Codd, C. T. Dillon, A. Levina and P. A. Lay, *Coord. Chem. Rev.*, 2001, **216/217**, 537–577.
- 3 S. A. Katz and H. Salem, in *The Biological and Environmental Chemistry of Chromium*, VCH Publishers, New York, 1994.
- 4 J. Barnhart, Chromium in Soil: Perspectives in Chemistry, Health, and Environmental Regulation: Special Issue, *J. Soil Contamination*, 1997, **6**, 561–568.
- 5 P. C. Grevat, *Toxicological Review of Hexavalent Chromium* (CAS No. 18540-29-9), U.S. Environmental Protection Agency, Washington DC, 1998.
- 6 X. Shi, A. Chiu, C. T. Chen, B. Halliwell, V. Castranova and V. Vallyathan, *J. Toxicol. Environ. Health, Part B*, 1999, 87–104.
- 7 M. Costa, *Crit. Rev. Toxicol.*, 1997, **27**, 431–442.
- 8 E. S. Gould, *Coord. Chem. Rev.*, 1994, **135/136**, 651–684.
- 9 D. K. Geiger, *Coord. Chem. Rev.*, 1997, **164**, 261–288.
- 10 A. Levina, P. A. Lay and N. E. Dixon, *Inorg. Chem.*, 2000, **39**, 385–395.
- 11 S. Signorella, C. Palopoli, M. Santoro, S. García, V. Daier, J. C. González, V. Roldán, M. I. Frascaroli, M. Rizzotto and L. F. Sala, *Res. Trends*, 2001, **7**, 197–207.
- 12 B. Gyuresik and L. Nagy, *Coord. Chem. Rev.*, 2000, **203**, 81–149.
- 13 M. Ciésłak-Golonka, *Polyhedron*, 1996, **15**, 3667–3689.
- 14 M. Rizzotto, A. Levina, M. Santoro, S. García, M. I. Frascaroli, S. Signorella, L. F. Sala and P. A. Lay, *J. Chem. Soc., Dalton Trans.*, 2002, 3206–3213.
- 15 V. Roldán, J. C. González, M. Santoro, S. García, N. Casado, S. Olivera, J. C. Boggio, J. M. Salas-Peregrin, S. Signorella and L. F. Sala, *Can. J. Chem.*, 2002, **80**, 1676–1686.
- 16 S. Signorella, R. Lafarga, V. Daier and L. F. Sala, *Carbohydr. Res.*, 2000, **324**(2) 127–135.
- 17 S. Signorella, M. I. Frascaroli, S. García, M. Santoro, J. C. González, C. Palopoli, N. Casado and L. F. Sala, *J. Chem. Soc., Dalton Trans.*, 2000, 1617–1623.
- 18 M. Rizzotto, V. Moreno, S. Signorella, V. Daier and L. F. Sala, *Polyhedron*, 2000, **19**, 417–423.
- 19 S. Signorella, V. Daier, S. García, R. Cargnello, J. C. González, M. Rizzotto and L. F. Sala, *Carbohydr. Res.*, 1999, **316**, 14–25.
- 20 S. Signorella, S. García and L. F. Sala, *J. Chem. Educ.*, 1999, **76**, 405–408.
- 21 V. Daier, S. Signorella, M. Rizzotto, M. I. Frascaroli, C. Palopoli, C. Brondino, J. M. Salas-Peregrin and L. F. Sala, *Can. J. Chem.*, 1999, **77**, 57–64.
- 22 M. Rizzotto, M. I. Frascaroli, S. Signorella and L. F. Sala, *Polyhedron*, 1996, **15**, 1517–1523.
- 23 S. Signorella, M. Rizzotto, V. Daier, M. I. Frascaroli, C. Palopoli, D. Martino, A. Boussecksou and L. F. Sala, *J. Chem. Soc., Dalton Trans.*, 1996, 1607–1611.
- 24 M. Rizzotto, S. Signorella, M. I. Frascaroli, V. Daier and L. F. Sala, *J. Carbohydr. Chem.*, 1995, **14**, 45–51.
- 25 L. F. Sala, C. Palopoli and S. Signorella, *Polyhedron*, 1995, **14**, 1725–1730.
- 26 L. F. Sala, S. Signorella, M. Rizzotto, M. I. Frascaroli and F. Gandolfo, *Can. J. Chem.*, 1992, **70**, 2046–2052.
- 27 S. Signorella, M. Santoro, C. Palopoli, C. Brondino, J. M. Salas-Peregrin, M. Quirós and L. F. Sala, *Polyhedron*, 1998, **17**, 2739–2749.
- 28 S. Signorella, S. García and L. F. Sala, *Polyhedron*, 1997, **16**, 701–706.
- 29 S. R. Signorella, M. I. Santoro, M. N. Mulero and L. F. Sala, *Can. J. Chem.*, 1994, **72**, 398–402.
- 30 B. Manuza, S. Deiana, M. Pintore and C. Gessa, *Carbohydr. Res.*, 1997, **300**, 85–88.
- 31 M. Branca and G. Micera, *Inorg. Chim. Acta*, 1988, **156**, 61–65.
- 32 R. Bramley, J.-Y. Ji, R. J. Judd and P. A. Lay, *Inorg. Chem.*, 1990, **29**, 3089–3094.
- 33 J. K. Beattie and G. P. Haight, in *Inorganic Reaction Mechanisms*, Part II, ed. J. O. Edwards, Wiley, New York, 1972.
- 34 M. Mitewa and P. Bontchev, *Coord. Chem. Rev.*, 1985, **61**, 241–272.
- 35 S. L. Scott, A. Bakac and J. H. Espenson, *J. Am. Chem. Soc.*, 1991, **113**, 7787–7788.
- 36 S. Scott, A. Bakac and J. Espenson, *J. Am. Chem. Soc.*, 1992, **114**, 4205–4213.
- 37 A. Al-Ajlouni, A. Bakac and J. H. Espenson, *Inorg. Chem.*, 1994, **33**, 1011–1014.
- 38 J. Pérez Benito, C. Arias and D. Lamrhari, *New J. Chem.*, 1994, **18**, 663–666.
- 39 J. Pérez Benito and C. Arias, *Can. J. Chem.*, 1993, **71**, 649–655.
- 40 C. Palopoli, S. Signorella and L. F. Sala, *New J. Chem.*, 1997, **21**, 343–348.
- 41 G. P. Haight, G. M. Jursich, M. T. Kelso and P. J. Merrill, *Inorg. Chem.*, 1985, **24**, 2740–2746.

- 42 R. G. Wilkins, *The Study of Kinetics and Mechanism of Reactions of Transition Metal Complexes*, Allyn and Bacon: Boston, 1974, pp. 20–23.
- 43 M. C. Ghosh and E. S. Gould, *Inorg. Chem.*, 1991, **30**, 491–494.
- 44 R. Codd, P. A. Lay and A. Levina, *Inorg. Chem.*, 1997, **36**, 5440–5448.
- 45 SigmaPlot for Windows, *Exact Graphs for Exact Science*, version 5.00, SPSS Inc., 1999.
- 46 S. Signorella, J. C. González and L. F. Sala, *J. Argentine Chem. Soc.*, 2002, **90**, 1–19.
- 47 G. Barr-David, M. Charara, R. Codd, R. P. Farrell, J. A. Irwin, P. A. Lay, R. Bramley, S. Brumby, J.-Y. Ji and G. R. Hanson, *J. Chem. Soc., Faraday Trans.*, 1995, **91**, 1207–1216.
- 48 M. Branca, A. Dessi, H. Kozłowski, G. Micera and J. Swiatek, *J. Inorg. Biochem.*, 1990, **39**, 217–226.
- 49 R. P. Farrell, R. J. Judd, P. A. Lay, R. Bramley and J.-Y. Ji, *Inorg. Chem.*, 1989, **28**, 3401–3403.
- 50 R. Codd and P. A. Lay, *J. Am. Chem. Soc.*, 1999, **121**, 7864–7876.
- 51 S. P. Kaiwar, M. S. S. Raghavan and C. P. Rao, *Carbohydr. Res.*, 1994, **256**, 29–40.
- 52 M. L. Ramos, M. M. Caldeira and V. M. Gil, *Carbohydr. Res.*, 1996, **286**, 1–15.
- 53 M. L. Ramos, M. M. Caldeira and V. M. Gil, *J. Chem. Soc., Dalton Trans.*, 2000, 2099–2103.
- 54 V. P. Roldán, V. A. Daier, B. Goodman, M. Santoro, J. C. González, N. Calisto, S. Signorella and L. F. Sala, *Helv. Chim. Acta*, 2000, **83**, 3211–3228.
- 55 M. Krumpolc and J. Rocek, *Inorg. Synth.*, 1980, **20**, 63–65.
- 56 S. Signorella, S. García and L. F. Sala, *Polyhedron*, 1992, **11**, 1391–1396.
- 57 O. A. Babich and E. S. Gould, *Inorg. Chem.*, 2001, **40**, 5708–5710.
- 58 N. E. Brasch, D. A. Buckingham, A. B. Evans and C. R. Clark, *J. Am. Chem. Soc.*, 1996, **118**, 7969–7980.
- 59 International Agency for Research on Cancer (IARC), *IARC Monogr. Eval. Carcinog. Risk Chem. Hum. Suppl.*, 1987, **7**, 165–168.
- 60 R. Feldam, *Occupational and Environmental Neurotoxicology*, Lippincott-Raven Publishers, Philadelphia, PA, 1999, pp. 337–338.
- 61 *Handbook of Chemistry and Physics*, CRC Press Inc., Boca Raton, FL, 68th edn., 1987–1988, p. C-710.
- 62 A. B. P. Lever, *Inorganic Electronic Spectroscopy*, Elsevier, Amsterdam, 2nd edn., 1984, p. 419.
- 63 *WinSIM EPR calculations for MS-Windows*, version 0.96: National Institute of Environmental Health Sciences, 1995.